J. Geomag. Geoelectr., 28, 85–97, 1976

Tectonomagnetic Experiments and Observations in Western U.S.A.

M.J.S. JOHNSTON, B.E. SMITH, and R. MUELLER

National Center for Earthquake Research,
U.S. Geological Survey,
Menlo Park, California, U.S.A.

(Received December 24, 1975)

Simultaneous measurements of the geomagnetic field with differential proton magnetometers (0.25 gamma sensitivity) have been recorded periodically since 1973 at more than 100 pairs of sites, 8 to 12 km apart, along active faults in western U.S.A. Along one 80 km test section of the San Andreas fault the data from 7 instruments is continuously telemetered to Menlo Park, California. Probable tectonomagnetic effects with amplitudes of about 1 and 1.8 gammas have been observed for earthquakes with magnitudes 4.2 and 5.2 respectively. The corresponding stress changes for simple dislocation models are in the range 10 and 100 bars respectively. Magnetic and electrical response differences and site separation appear to be the most important factors determining discrimination limits for tectonomagnetic signals.

1. Introduction

Active faults in the western U.S.A., although potentially dangerous in terms of a threat to life and property, do provide a unique opportunity for studying the earthquake process. The most important unmonitored parameter in this process is the change in crustal stress associated not only with earthquakes in the periods preceding, during, and following the event but also with aseismic slip on the fault.

This paper discusses several experiments in progress in this region whose design is based on the concept that piezomagnetic changes should occur in crustal rocks. The results obtained are discussed in terms of whether these measurements monitor stress changes related to regional strain accumulation and/or the occurrence of earthquakes.

2. Tectonomagnetic Effects

Tectonomagnetic effects arise primarily from the stress induced magnetic anisotropy in crustal rocks that contain grains of magnetic mineral (KERN, 1961;

STACEY, 1962; NAGATA, 1966; STACEY and JOHNSTON, 1972). The techniques necessary and the problems encountered in attempting to observe these effects are discussed by RIKITAKE (1966a, b), JOHNSTON *et al.* (1973), and JOHNSTON (1974). Calculated tectonomagnetic anomalies for models of the most well-known faults have been attempted by STACEY (1964), SHAMSI and STACEY (1969), TALWANI and KOVACH (1972), and HILDEBRAND and BHATTACHARYYA (1974).

Most of the relative displacement between the Pacific and North American plates appears to be localized within the San Andreas fault system in western U.S.A. (SAVAGE and BURFORD, 1973). Moderate seismicity is common in this region (as illustrated in Fig. 1) with most earthquakes having focal depths less than 10 km. It must be presumed that, due to both the systematic right lateral shear and the strain release due to earthquakes and aseismic slip, stress changes are occurring in this region.

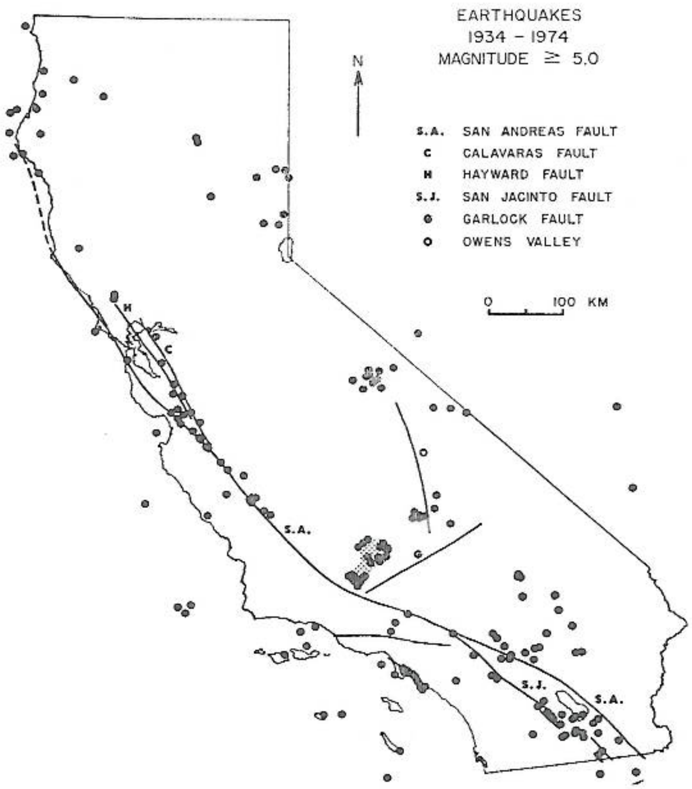

Fig. 1. Some important active faults in California and the location of earthquakes of magnitude greater than 5.0 during the past 40 years (unpublished data, 1974, U.S. Geological Survey).

3. Tectonomagnetic Experiments and Observations

The necessary prerequisites for the successful observation of tectonomagnetic effects are a high stress sensitivity of rock magnetization and favorable location of a highly stable and sensitive measuring system. Unfortunately, little is known of either the location and spatial extent of dynamic stress fields on active faults or the volume, geometry, and magnetization at relevant depths of magnetic rocks. Crude indications of the distribution of rock magnetizations can be derived from surface sampling and aeromagnetic maps. However, in the absence of any real observations of the form and spatial extent of stress fields, the location of magnetometer sites so as to optimize signal amplitude has usually been determined on the basis of theoretical dislocation models of the earthquake process.

On the San Andreas fault system, synchronized proton magnetometers of 0.25 gamma sensitivity are being used both in a fixed station array and in a

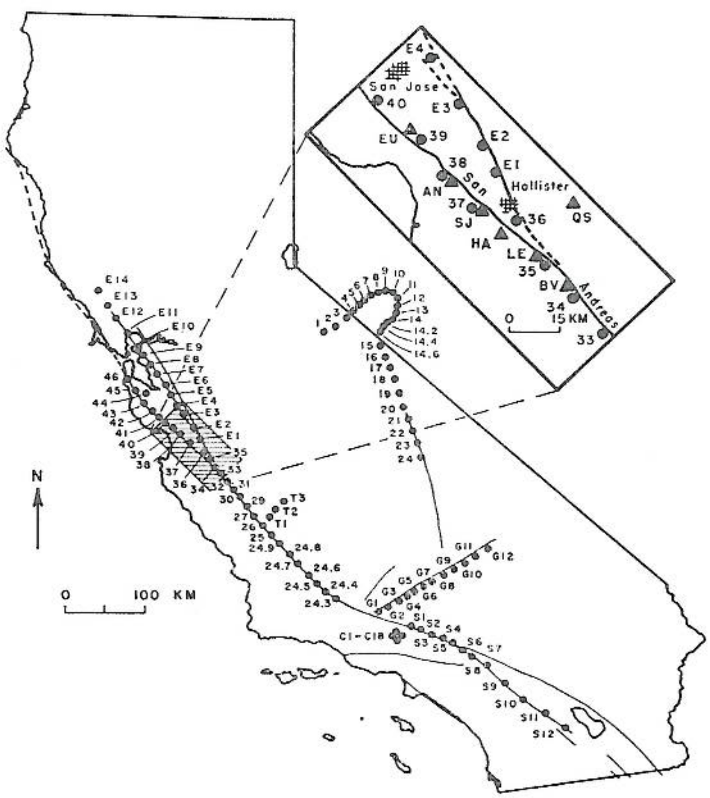

Fig. 2. Location of periodically resurveyed (dots) and permanent magnetometer sites (triangles in the expanded section) in California and Nevada.

portable resurvey mode to determine the existence and characteristics of these effects. As discussed by JOHNSTON (1974), the primary aim of the resurvey experiment is to identify large scale long period effects that could provide an indication of an impending earthquake in a poorly instrumented area. Regional baseline data obtained this way is also compared with data taken subsequent to any large earthquakes and calibrated where possible in control experiments using known crustal loads due to dams (DAVIS and STACEY, 1972; JOHNSTON *et al.*, 1973).

Data have been obtained in the resurvey experiment at pairs of sites approximately 10 km apart along 1200 km of active faults in California and Nevada. The locations of these sites are shown on the map in Fig. 2. Surface rocks samples were collected at most of the sites and their magnetizations range from 3×10^{-3} to 10^{-6} e.m.u. Although there appears to be a general correspondence between these values and details of the aeromagnetic map of the fault (HANNA *et al.*, 1972), the development of a relation between earthquakes and anomalies in a particular region will be largely empirical unless stress and magnetization heterogeneity is found to be minor. The regions in Fig. 2 where measured magnetizations exceed 10^{-4} e.m.u. are near sites S10, G4 to G6, G9, 3 to 14.6, 19 to 21, 24.8 to 25, 34, 37, 38, and E11 to E14.

The areas of most interest are those where crustal stress is probably concentrated and perhaps increasing and also where the magnetizations of the rocks are high. Such areas are perhaps near San Juan Bautista (Site 37; 36°48′N, 121°32′W), Bear Valley (Site 34; 36°35′N, 121°12′W), Cholame (Site 25; 35°50′N, 120°20′W), Garlock (Site G9; 35°15′N, 117°45′W), and the Excelsior Mountains (Sites 4 to 15; 38°20′N, 118°15′W) in Nevada. It is interesting to note, by comparing Fig. 1 and Fig. 2, that the regions of highest seismicity also have the most magnetic rocks. While generally true for global scale tectonics, occurrence on this scale also, although probably for different reasons, is intriguing.

At each pair of adjacent sites, a set of about 75 total field values are recorded in a 10-minute period during the times when the geomagnetic field is relatively undisturbed. The magnetometers are synchronized by reference clocks and/or by radio. The data are later used to generate mean differences and standard deviations of these differences. The largest standard deviation for a single set of data was 1.5 gammas. The standard deviation in 10-minute averages of total field differences for a 10 km site separation is being determined with an array of continuously recording fixed station magnetometers. Preliminary data indicate a value of less than two gammas. The change with time in 10-minute means of local field differences is considered to be significant (at the 95 per cent confidence level) only if it exceeds 3.5 gammas.

The variations with time of resurveyed local magnetic field changes that have occurred along 250 km of the San Andreas fault from October 1972 to

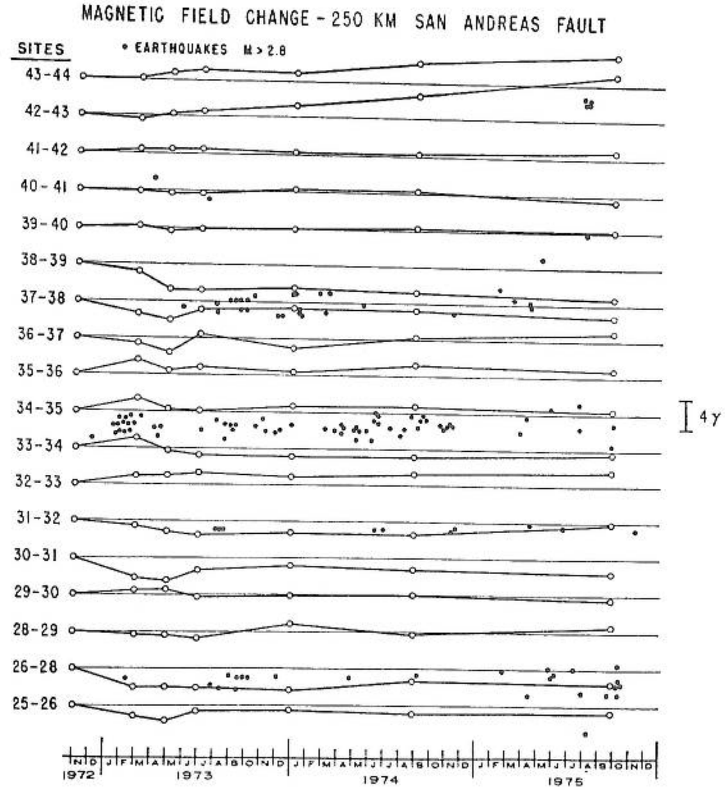

Fig. 3a. Local magnetic field change with time between Site 24.9 and Site 44 (Fig. 2) along 250 km of the San Andreas fault. The approximate location and occurrence time of earthquakes with magnitudes greater than 2.8 are marked with dots.

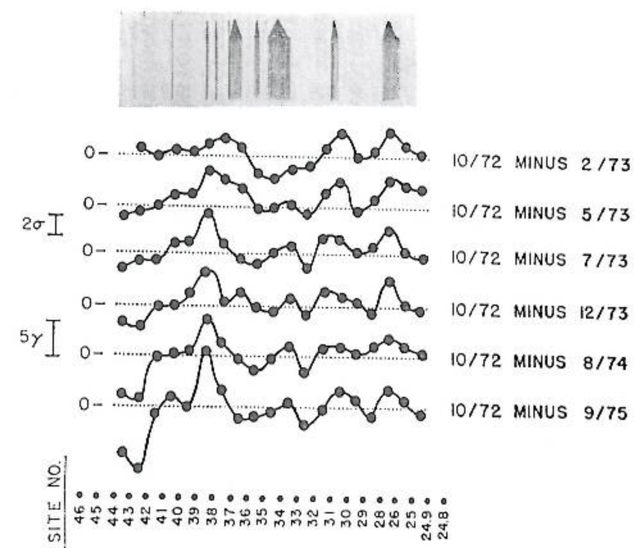

Fig. 3b. Change in local magnetic field differences between successive surveys along the San Andreas fault. The occurrence times of earthquakes with magnitudes greater than 2.8 are shown as vertical lines (after JOHNSTON, 1974).

September 1975 are shown in Fig. 3a. Also included are earthquakes of magnitudes greater than 2.8 that occurred in this area during this time. This plot shows data from seven complete runs along the section of the San Andreas fault between Sites 24 and 44 (Fig. 2) that covers the first three regions of interest and overlaps the section of fault that is continuously monitored with the fixed station array.

The important features of this plot are as follows:

a) Regions with the greatest local magnetic field change coincide generally with regions of high/moderate seismicity. An exception to this is for Sites 42, 43, and 44 where a systematic change has occurred since mid-1973 with little associated seismicity. Some more detailed monitoring has therefore been planned for this area. The relation between anomalies and seismicity is better illustrated by the change in local magnetic field as a function of spatial position since the first survey. Figure 3b is a plot updated from JOHNSTON (1974) which shows the local field change as a function of site pair location subsequent to the first survey. The vertical lines represent earthquakes with magnitudes greater than 2.8.

b) The largest changes are only marginally above the noise level (Fig. 3b). However, most of these changes for the independent data sets are generally in the same sense, at the same sites, and therefore are less likely to be due to noise.

c) Earthquakes that occurred within 10 km of a site had magnitudes less than 3.6 and source dimensions less than 1 km. The dimensions of the anomalies exceeds in some cases the site separation. This would indicate that these small earthquakes are only a symptom of a larger scale process.

A similar data set from sites in the Owens Valley–Excelsior Mountains area (Fig. 2) is plotted in Fig. 4. The northern part of the region is important since the surface rocks have magnetizations of approximately 10^{-3} e.m.u. and the seismicity is high (PRIESTLEY, 1975). In contrast, the southern section (Sites 18 to 24) is relatively aseismic although a magnitude 8.3 earthquake did occur at Site 24 in 1872. The largest magnetic changes since 1973 evident in Fig. 4 occur near the eastern and western edges of the Excelsior Mountains (Site 8 and 14 respectively) and the western side of the Mono basin (Site 4). Little change is observed from Sites 18 to 24. Since Sites 17 to 24 are in a presently aseismic region, the data could serve to indicate, in comparison with data from active regions such as the San Andreas, what the character and noise in data for parallel experiments in an aseismic region would look like.

The best indication that earthquake related magnetic field changes are being monitored with the survey technique occurred with several earthquakes in June 1974 on the Garlock fault. These earthquakes ($M=3.8$ to 4.3) were the largest that had occurred within five kilometers of a survey site.

On May 16, 1974, the first data were taken at Sites G1 to G12 (Fig. 1).

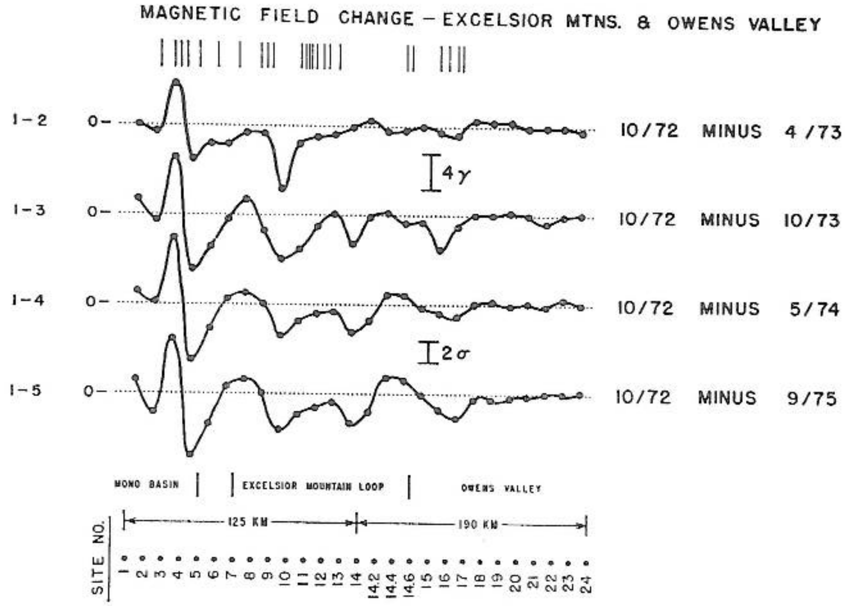

Fig. 4. Local magnetic field change as a function of location in the Mono Lake–Excelsior Mountains–Owens Valley region. Earthquakes plotted from PRIESTLEY (1975) with magnitudes greater than about 3.0.

The earthquakes occurred on June 9 and June 10 within five kilometers of G9. The survey was repeated two weeks after the earthquakes and again three months later. Figure 5, from JOHNSTON *et al.* (1975), shows that the data following the earthquake at G9 changed relative to the pre-earthquake values. As reported by JOHNSTON *et al.* (1975), this would result from an increase in the local field at G9. After three months the same general form of anomaly still remained although spatially expanded such as might occur if stress field discontinuities became more dispersed. A one gamma change is consistent with the field calculated from a dislocation model with slip 2 km in extent at the earthquake hypocenter if the product of stress change and magnetization is about 0.01 e.m.u. bars. The range of magnetization of surface rocks collected at G9 is from 10^{-4} to 10^{-3} e.m.u. This implies in such a simple although poorly constrained model, a stress change of between 100 and 10 bars respectively.

A seven-station array of continuously operating magnetometers (SMITH *et al.*, 1974) is installed along the 80 km section of the San Andreas shown in Fig. 1. This section is presently one of the most seismically active parts of the San Andreas. Survey sites in this region are shown also in the expanded section of Fig. 2. The instruments sample simultaneously once a minute and the data are telemetered digitally to Menlo Park, California, and recorded.

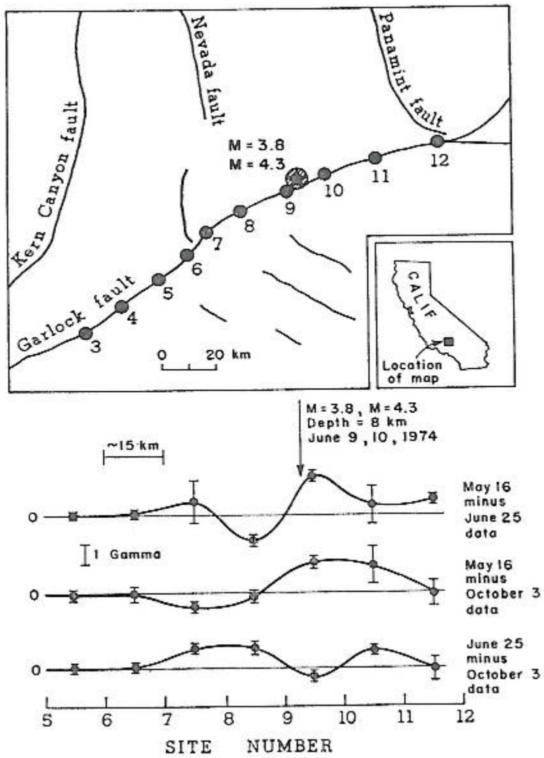

Fig. 5. Simplified fault map showing magnetometer sites and earthquake locations along the Garlock fault, California. Magnetic field changes as a function of site location are plotted for the periods May 16 to June 25, May 16 to October 3, and June 25 to October 3, 1974. Earthquakes of magnitude $M=3.8$ and 4.3 occurred on June 9 and June 10. The error bars represent one standard deviation of individual values about a mean of 75 values (after JOHNSTON *et al.*, 1975).

Five-day running mean differences for each consecutive station pair are shown in Fig. 6. The error bars on each plot correspond to two standard deviations of the data. Any tectonic signals that are included will tend to give an overestimate of the noise. Subgamma discrimination does appear possible in this period range at all sites except the two most northern.

Also included on Fig. 6, plotted as triangles, are the magnetic field differences determined by the survey experiment. Since the field sites for the two experiments do not coincide, the survey data are plotted with the data for the station pair that corresponds most closely with the survey sites. There is a surprisingly good correspondence between the two data sets considering the different sample interval and size. An exception is the April 1974 survey data corresponding to SJ-HA.

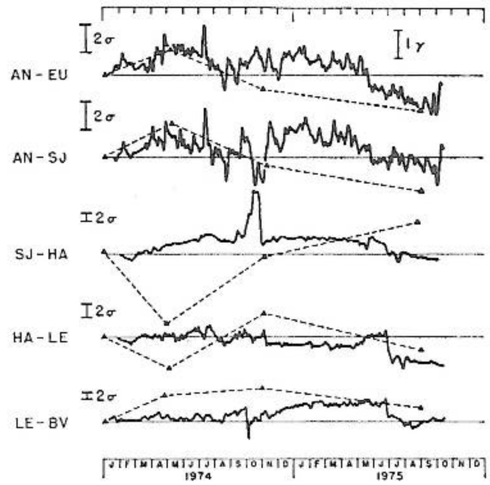

Fig. 6. Comparative plot of survey data (dashed record) and five-day running mean differences between consecutive pairs of continuously monitored stations from January 1974 to September 1975. The error bars represent two standard deviations about the five day means calculated from detrended data for each station pair during seismically quiet times.

The most significant change recorded in 18 months since January 1, 1974, was observed on SJ-HA in October 1974 about a month before the largest earthquake to occur in this region during this period—a magnitude 5.2 earthquake on November 28, 1974. Details of these results have been discussed by SMITH and JOHNSTON (1976).

With the exception of this earthquake, the earthquakes that occurred within 10 km of an operating magnetometer, had magnitudes of up to 3.6. No clear relation is evident between these earthquakes and local magnetic field changes. With so few unambiguous observations associated with earthquakes it is difficult to assess the merits and limitations of this technique for earthquake prediction. It is therefore hard to justify the next stage of this experiment to determine details of the stress field change and scale by instrumenting with three-component magnetometers and inverting the data using standard inversion techniques.

In order to detect changes from these smaller magnitude earthquakes it will be necessary to understand and reduce further the background noise in the differential magnetometer measurements. Table 1 lists some of the most common signal (noise) source processes in differential magnetometer measurements. It is obvious that many of these processes are interrelated and it is the effects of, for example, differences in average susceptibility, conductivity, or main field vector directions, etc. that reduce cancellation of ionospheric and magnetospheric

Table 1. Magnetic signals in scalar differential magnetometer measurements.

Process	Probable field amplitude on 10 km baseline scalar differential magnetometers	Primary period range
A) External fields; dispersed ionospheric and magnetospheric sources incompletely cancelled with a 10 km baseline	~Up to 10 gammas	Short periods diurnal and solar periods
B) Internal fields:		
1) Externally induced internal currents	~Several gammas	Primarily short period
2) Susceptibility differences between sites	~Several gammas	Short period, diurnal, and solar periods
3) Differences in total magnetization directions between sites	~Several gammas	All periods
4) Thermal magnetization or demagnetization	A few gammas/year in volcanic regions; much less elsewhere	Smooth long term trend
5) Secular variation	~Several gammas in several years, generally much less	Smooth long term trend
6) Magnetohydrodynamic	Potentially a few gammas spatially localized in volcanic regions, insignificant elsewhere	Short period
7) Piezomagnetic effects	A few gammas in regions with substantial stress change (~50 bars) and moderate magnetizations ($\lesssim 10^{-3}$ e.m.u.)	Reflects time dependence of stress field

disturbances in simple differences. The important initial task is to rank these effects in general and in detail for each instrument pair.

Initial noise analysis indicates that there are two main noise effects. Firstly, there is small amplitude, high frequency incoherent noise with about 0.5 gamma standard deviation present in all differences at all times. The random or "gaussian" character of this noise makes it easy to reduce by simple averaging techniques. Superimposed on this are larger amplitude, generally coherent low frequency sporadic noise clearly related to ionospheric and magnetospheric disturbances. The amplitudes of these disturbances on each difference appears to be primarily a function of station separation, susceptibility contrast, and conductivity structure. Initial results indicate that the first two appear to be the most effective, particularly at longer periods. An estimate of the effect of susceptibility contrast is obtained by selecting pairs of sites with approximately the same site separation but different values of susceptibility difference. For data taken during the same time period, enhanced standard deviations of daily mean differences ($\Delta\sigma_\chi$ gammas) as a function of susceptibility difference ($\Delta\chi$) for $\Delta\chi >$ 10^{-4} e.m.u. can be represented by the equation

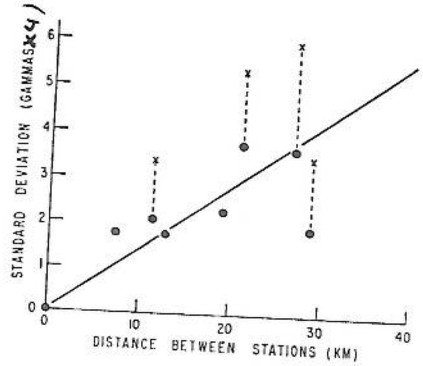

Fig. 7. Standard deviation of daily mean differences as a function of site separation (crosses). The data are replotted (dots) after being corrected for the effect of susceptibility differences.

$$\Delta\sigma_\chi = \overset{0.2}{\cancel{0.6}} \log \Delta\chi + \overset{1.1}{\cancel{3.8}} .$$

Standard deviations of daily mean differences (crosses) as a function of site separation (D) are plotted in Fig. 7. The same data are replotted (dots) after being corrected for the effect of susceptibility differences. The best linear relation between the corrected standard deviation (σ_c) and distance is given by

$$\sigma_c = \overset{0.03}{\cancel{0.14}} D .$$

The assessment of the effects of conductivity differences in this extremely complex geologic environment is much more difficult. The operation of pairs of portable component magnetometers at each site pair may give sufficiently stable transfer functions that some additional noise reduction will be possible. It is fortunate that this effect does not seem to be of prime importance even though some large scale enhanced vertical and horizontal components might be expected due to the general proximity to the ocean.

A detection capability at the 0.5 gamma level or slightly better for intermediate to long period tectonomagnetic effects does appear possible at most sites in this array. Shorter period effects (i.e., for a few minutes to a day) will be difficult to see unless they exceed three or four gammas.

4. Conclusions

Observation of total geomagnetic field along active faults in the western U.S.A. has been intensified since early 1973. The repeated magnetic surveying results indicate that fairly regular increases in local field occur in regions where seismicity is occurring or will subsequently occur. The scale of these changes is from one to two orders of magnitude greater than the largest earthquake source dimension. The best data, obtained for the largest earthquakes close to monitoring sites, indicate a crude causal relationship between local field change and earthquakes. Anomalous change has occurred in one region so far without substantial seismicity. Confidence in the usefulness of this technique will increase if this region becomes increasingly seismic. As an independent check and precaution in this area, surface monitoring using a small array of tiltmeters has been initiated.

In the region where the surveying experiment sites overlap the sites for continuous field monitoring, the data agree well within the anticipated noise limits.

Identical repeated surveying of several hundred kilometers of an aseismic region has yet to be completed in order to check whether the changes observed occur only in seismic areas. However, comparison of data obtained for more than one hundred kilometers in the lower aseismic part of the Owens Valley with that obtained on the San Andreas or in the Excelsior Mountains indicates peak-to-peak variations are up to a factor of four lower in the Owens Valley.

In the region continuously monitored with permanent magnetometers, significant changes in local field have been observed. The clearest anomaly occurred almost a month before the largest earthquake in this region since early 1973. In general, however, no unique relationship has been observed between other changes and the numerous occurrence of moderate magnitude earthquakes. No earthquakes with magnitudes greater than 3.6 have occurred within 10 km of a sensor. The magnitude threshold for generation of tectonomagnetic effects within the San Andreas fault zone is concluded to be greater than magnitude 3. Differences in magnetic induction and site separation appear to be the most important processes limiting detection of tectonomagnetic effects.

Little is known concerning stress changes, both seismic and aseismic, on active faults. The techniques discussed here for systematic observation of tectonomagnetic effects appear to provide a simple and economically feasible way to monitor these changes.

REFERENCES

DAVIS, P.M. and F.D. STACEY, Geomagnetic anomalies caused by a man-made lake, *Nature*, **240**, 348, 1972.

HANNA, W.F., R.D. BROWN, D.C. ROSS, and A. GRISCOM, Aeromagnetic reconnaissance and generalized geologic map of the San Andreas fault between San Francisco and San Bernardino, California, Geophys. Inv. Map GP-815, U.S. Geol. Survey, 1972.

HILDEBRAND, T.G. and B.K. BHATTACHARYYA, Seismomagnetic anomalies due to various dislocation models, *Trans. Am. Geophys. Union*, **56**, 1112, 1974.

JOHNSTON, M.J.S., Preliminary results from a search for regional tectonomagnetic effects in California and western Nevada, *Tectonophysics*, **23**, 267, 1974.

JOHNSTON, M.J.S., G.D. MYREN, N.W. O'HARA, and J.H. RODGERS, A possible seismomagnetic observation on the Garlock fault, California, *Bull. Seis. Soc. Am.*, **65**, 1129, 1975.

JOHNSTON, M.J.S., B.E. SMITH, J.R. JOHNSTON, and F.J.A. WILLIAMS, Search for tectonomagnetic effects in California and western Nevada, *Proc. Conf. on Tectonic Problems of the San*